

A Study of Atmospheric Boundary Layer (ABL) Height Estimation using Various Analytical Methods - COSMIC RO Measured Temperature Profiles

V. Naveen Kumar¹, P. S. Brahmanandam^{2*}, M. Purnachandra Rao³, G. Anil Kumar⁴,
K. Samatha³ and L. Rupa Dhanasri⁵

¹Department of Basic Science, Gudlavalleru Engineering College, Gudlavalleru - 521356, Andhra Pradesh, India; vangipurapu1980@gmail.com

²Department of Basic Science, Shri Vishnu Engineering College for Women, Bhimavaram - 534202, Andhra Pradesh, India; dranandpotula@svecw.edu.in

³Department of Physics, Andhra University, Visakhapatnam - 530003, Andhra Pradesh, India; raomp17@gmail.com, ksamatha.phy@auvsp.edu.in

⁴School of Renewable Energy and Environment, JNTUK, Kakinada - 533003, Andhra Pradesh, India; gorantlaanilkumar@gmail.com

⁵Department of ECE, Shri Vishnu Engineering College for Women, Bhimavaram - 534202, Andhra Pradesh, India; rupadhanasri@svecw.edu.in

Abstract

Objectives: Although several methods are available to identify ABL Height (ABLH), a comprehensive study on the usage of different analytical methods has not been reported widely, particularly on global databases. **Methods/Analysis:** In this research, we use various analytical methods including, gradient, double gradient and logarithmic gradient to estimate ABLH during two months (March and April 2013) period and applied those methods on COSMIC Radio Occultation retrieved temperature profiles to estimate ABLH. **Findings:** The estimated ABLHs are arranged in order to present them globally and diurnally that clearly show a few distinct features. Mainly, land and desert areas are associated with higher ABLH during daytime hours. Cold land areas (Arctic and Greenland) show relatively lower magnitudes and reverse are the cases with ABLH over cold oceans (Antarctic oceans). Most importantly, a distinctive diurnal feature is observed with a peak at sharp noon time and relatively lower values in the night time, which indicate both convective and stable layers, have evolved based on the ambient conditions that would exist during the day and nighttime ambient conditions. However, morning and evening transitions are not found in diurnal variations. **Applications/Improvements:** It is found that both gradient and logarithmic methods are able to find accurate ABLH, though still a great room exists to verify various other methods in finding ABLH.

Keywords: Atmospheric Boundary Layer Height, Analytical Methods, COSMIC RO Technique, Stable and Convective Layers

1. Introduction

The Atmospheric Boundary Layer (ABL), the lowest layer of the atmosphere near to the Earth's surface, is a highly dynamic layer that is, in general, influenced by various

parameters including, surface heating, turbulence, moisture transport and others.^{1,2} It is known that ABL exhibits strong diurnal variations mainly due to the exchange of energy and momentum between Earth's surface and the atmosphere and, hence, a proper knowledge of ABL depth

*Author for correspondence

and its fluctuations in time are essential for the estimation of the transport of atmospheric constituents.³⁻⁵ It is well known that the depth of the ABL varies daily in harmony with the thermal and frictional influence of the Earth's surface. As a consequence, ABL evolution is heavily dictated by thermal (solar heating) and mechanical (wind shear) turbulence. Further, ABL dynamics play a pivotal role in the vertical transport and mixing of aerosols from the surface of the Earth to the free troposphere.⁶⁻⁸

One can classify the diurnal pattern of ABL based on the different physical processes including the Convective Boundary Layer (CBL), the Stable Boundary Layer (SBL) and the Residual Layer² (RL). Out of these, the CBL develops during the daytime just after the sunrise due to convective turbulence associated with the entrainment zone, a stable layer, on its top. On the other hand, just before the sunset and during night time epochs, as the thermals cease to develop, the CBL crumbles and the SBL forms due to rapid cooling of the surface. Even though thermals stop to grow during nighttime, the mean state variables remain nearly the same as the former CBL, creating the RL associated with capping inversion layer, a stable layer, on its top.

Data collected from various remote sensing techniques and models have been effectively utilized to estimate ABLHs including, radiosondes,¹⁰⁻¹² wind profiles,^{13,14} LIDAR,^{15,16} GPS-based Radio Occultation techniques¹⁷⁻¹⁹ and ECMWF model.^{20,21} As fate would have it, there are certain advantages and disadvantages to the so-called remote sensing instruments and models. At the outset, radiosonde, a balloon-borne telemetry instrument ascends into the atmosphere, is one of the earliest remote sensing techniques that used to measure altitude, temperature, humidity and pressure with unprecedented vertical resolutions (~30 meters) upto 30 km. However, it would be a tougher or impossible job to maintain global coverage of radiosondes particularly over the ocean regions, as a typical radiosonde station needs to have a ground-tracking station and a consequence, a global picture of ABLH is nearly impossible to obtain with radiosondes.

As far the global features of ABLH are concerned, nearly similar problems do exist with LIDAR and wind profiles, though the vertical resolution and altitude coverage are entirely different for these remote sensing instruments. ECMWF model also, often times, unable to find a few important global and local phenomena, most

probably due to the huge averaging of internal variability of reanalysis databases.^{22,23} On the other hand, a constellation six micro-satellites, named COSMIC (Constellation Observing System for Meteorology, Ionosphere and Climate) Radio Occultation (RO) technique is able to collect global lower atmosphere (bending angle, refractivity, temperature and water vapor) and ionospheric profiles (electron densities) with unprecedented vertical and horizontal resolutions from 15 April 2006 onwards. Several important research studies were carried-out using COSMIC RO retrieved atmospheric and ionospheric regions.²⁴⁻²⁶ This study has also utilized various analytical techniques on COSMIC RO retrieved temperature profiles to present global (Longitude vs. Latitude) and diurnal (Local time vs. Latitude) variations of ABLH.

The grouping of this paper is as follows: The Section 1 will have a brief introduction and that also provides the motivations to carry-out this research work. In Section 2, it is presented the detailed data analysis procedure and methodologies, respectively. Section 3 will contain the observational results and discussion part. The needs of the future works are emphasized in Section 4. The conclusions are summarized in Section 5, which follows the acknowledgment and reference sections.

2. Data and Methodology

After downloading two months (March and April 2013) RO data from the COSMIC website <https://cdaac-www.cosmic.ucar.edu>, various analytical methods were applied to the downloaded data to estimate ABLH. In general, ABLH is determined using the parcel method or Gradient Method (in which ABLH is determined based on the presence of gradients of temperature and humidity profiles²⁷). The Gradient Method has been effectively used to estimate ABLH from the potential temperature profiles. In this method, the ABLH is estimated by finding the height corresponding to the maximum in the first derivative of the potential temperature profile³ and various researchers have effectively used Gradient Method to find ABLH height.^{28,29} The double Gradient Method estimates ABLH by finding the second derivative of the potential profile and this method is more effective one when small gradients do exist in the boundary layer. Last, not the least, the logarithmic method estimates ABLH at the altitude where the minimum of the logarithm of the first gradient of potential temperature is reached.³⁰

3. Observations and Discussion

We have, randomly, selected a few temperature profiles around the globe and have applied various differential methods (gradient, double gradient and logarithmic gradient) on the selected profiles to estimate ABLHs at various geographical locations. Figures 1 to 3 show the estimated ABLH during nighttime (2300 local time, LT), daytime (1100 LT) and nighttime (0200 LT) hours, respectively, over oceanic regions and the estimated ABLHs are shown in the figure itself. It is clear from these figures that both gradient and logarithmic gradient are showing very similar values, and hence, performed well in locating ABLH when compared to the double gradient method.

Since our aim is to present the global and diurnal variations of ABLH, one expects a good number of COSMIC RO occultation points during the study period (March and April 2014) globally. We, therefore, present the number of occultations provided by the COSMIC RO technique in the following lines. Figures 4 and 5 show the number of occultation points during March 2014 (61,682) and April 2014 (55,169) and these are around 2,050 and 1,840 profiles per day. Interestingly, a good number of profiles can be seen between middle and higher latitudes as the inclination angle for COSMIC micro-satellites is 71 degrees.³¹

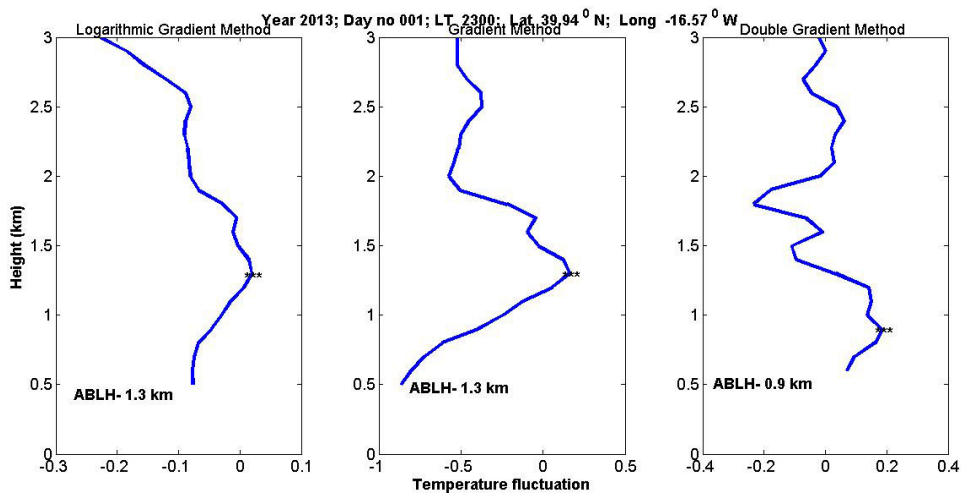


Figure 1. Estimation of ABLH using various analytical methods including, logarithmic gradient, gradient and Double Gradient Method in January 01, 2013 at 2300 local time.

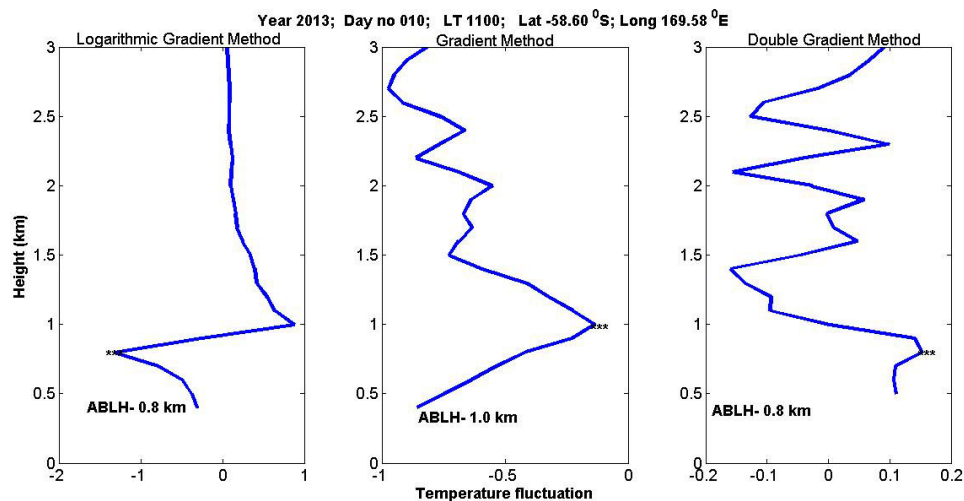


Figure 2. Estimation of ABLH using various analytical methods including, logarithmic gradient, gradient and Double Gradient Method in January 10, 2013 at 1100 local time.

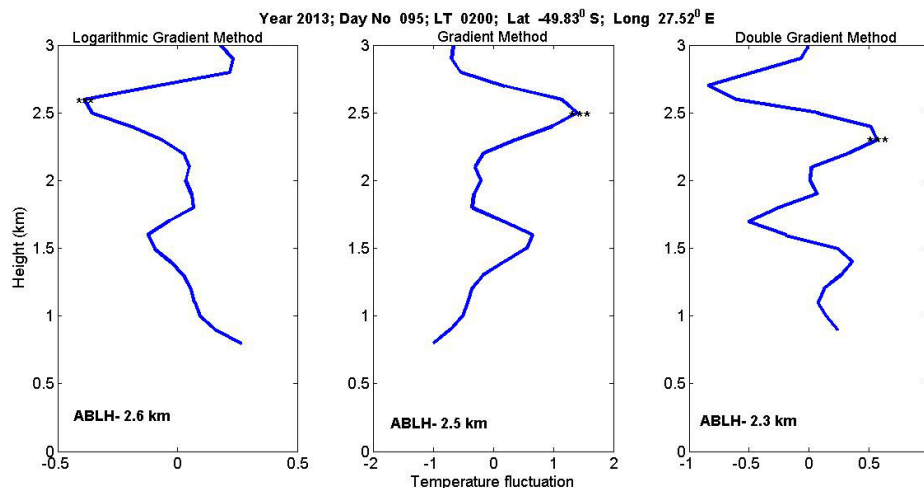


Figure 3. Estimation of ABLH using various analytical methods including, logarithmic gradient, gradient and Double Gradient Method in April 05, 2013 at 0200 local time.

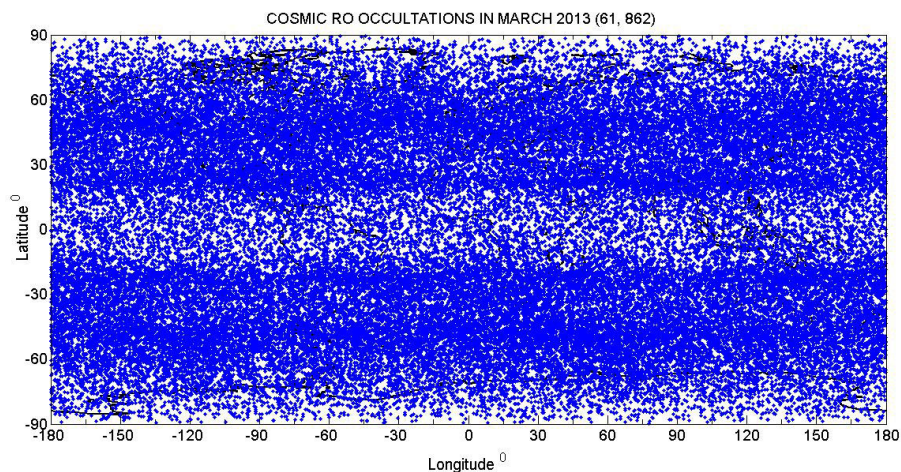


Figure 4. COSMIC RO occultations in March 2013 (61, 862), on average ~2,050 profiles are available per day,

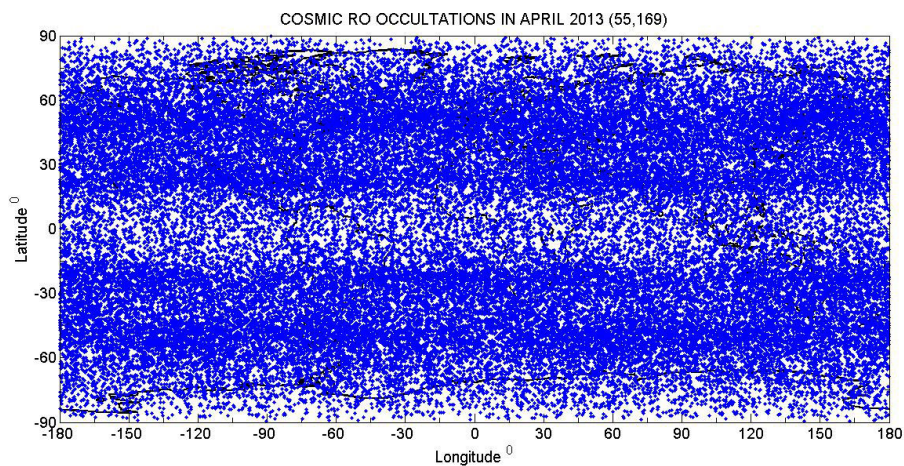


Figure 5. COSMIC RO occultations in April 2013 (55,169), on average only ~1, 840 profiles per day are available,

3.1 Global variations

Figures 6 (a, b,c) show global variations of ABLH during daytime (1000 LT-1400 LT) in March 2013 estimated using gradient, double gradient and the logarithmic gradient methods, respectively. Note that we have applied effective averaging and smooth techniques to avoid a few uneven ABLH values and have, therefore, kept ABLH magnitudes between 0 and 3000 meters only. It may be worth mentioning here that the similar procedure is also applied for ABLH when we present them in April 2013 as well as for diurnal variations.

A mere look at Figures 6a, 6b and 6c show a few distinctive features that need to be evaluated in a careful way in order to understand the physical phenomenon behind them. For example, both gradient and logarithmic gradient methods provide (Figures 6a and 6b) higher ABLH magnitudes (~between 2000-3000 meters) over land areas in the majority of the regions: Be it Americas, Asian, Africa, European and Australians regions. It has been reported that ABLH over land areas is higher in the absence of any upper level cloud and when surface temperatures are higher.³² A clear examination of these figures also shows desert regions are associated with higher magnitudes, though a few fluctuations in higher magnitudes could be seen here and there (Patagonian and Sahara desert regions).

Further, cold land regions (Arctic and Greenland regions) show too meager magnitudes (~500 meters only), whereas the Antarctic region depicts irregular structures and relatively higher magnitudes which we do not understand. The majority of observational findings that we have reported here is in great consistency with the climatology of ABLH derived using the ECMWF re-analysis.²⁰ We also present global variations of ABLH during April 2013 in Figures 7 (a, b, c) using gradient, double gradient and logarithmic gradient methods. Almost, near-similar results are found that we report for the ABLH during March 2013, which include higher magnitudes over land and desert regions and relatively meager magnitudes over cold land regions (Arctic and Greenland regions) and irregular structures and relatively higher magnitudes over the Antarctic region. Further, great consistencies can clearly be seen in ABLH estimated using gradient and logarithmic gradient methods. Though global ABLH estimated using gradient and logarithmic gradient methods show near similarities with each other and with earlier results, no such similarity is found in the ABLH estimated using the double Gradient Method during March and April 2013, which means that the double gradient may not be useful in delineating ABLH derived from COSMIC RO retrieved atmospheric products.

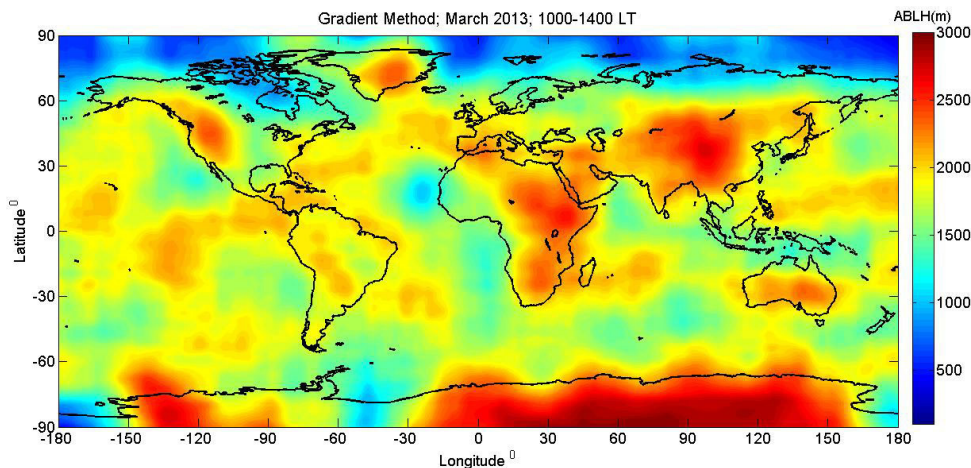


Figure 6a. Daytime (1000-1400 LT) trends of ABLH in March 2013, which are computed based on the Gradient Method (GM).

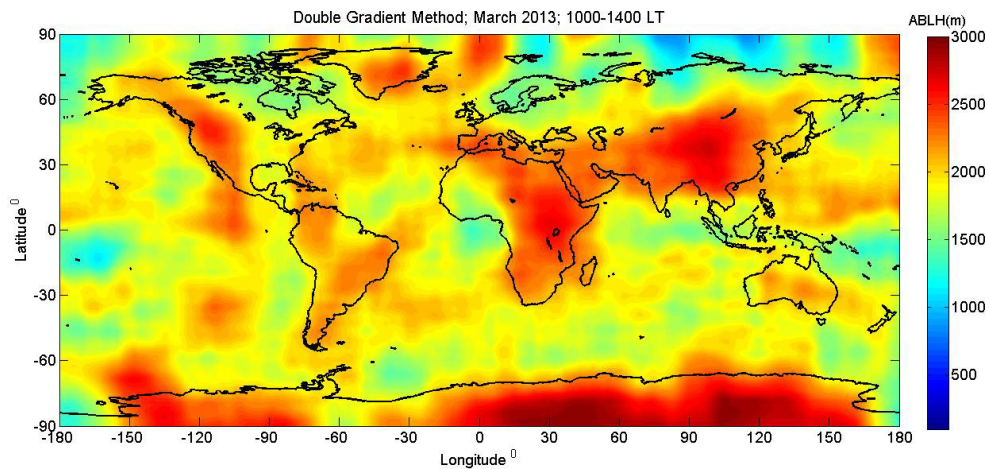


Figure 6b. Daytime (1000-1400 LT) trends of ABLH in March 2013, which are computed based on the Double Gradient Method (DGM).

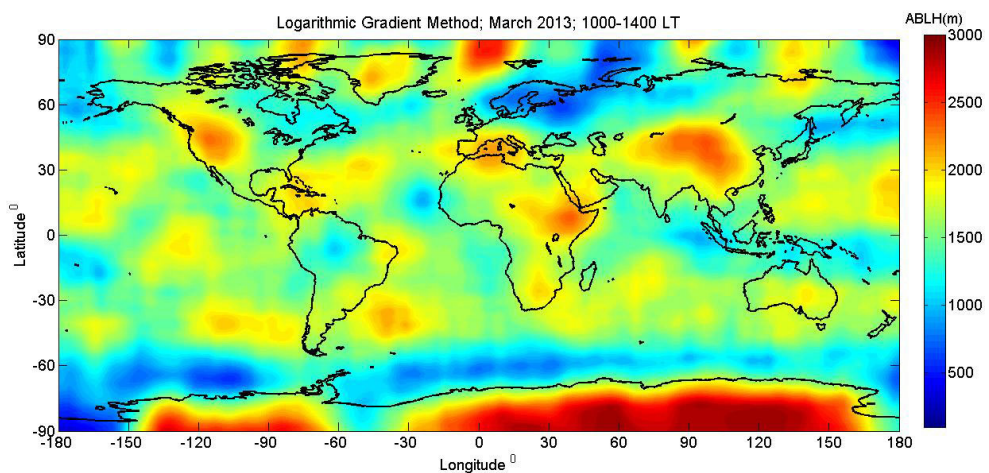


Figure 6c. Daytime (1000-1400 LT) trends of ABLH in March 2013, which are computed based on the Logarithmic Gradient Method (LGM).

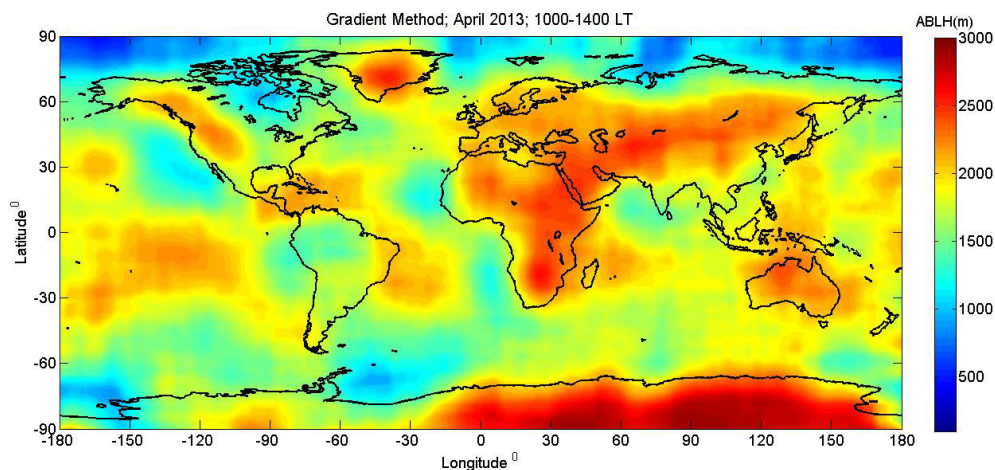


Figure 7a. Daytime (1000-1400 LT) trends of ABLH in March 2013, which are computed based on the Gradient Method (GM).

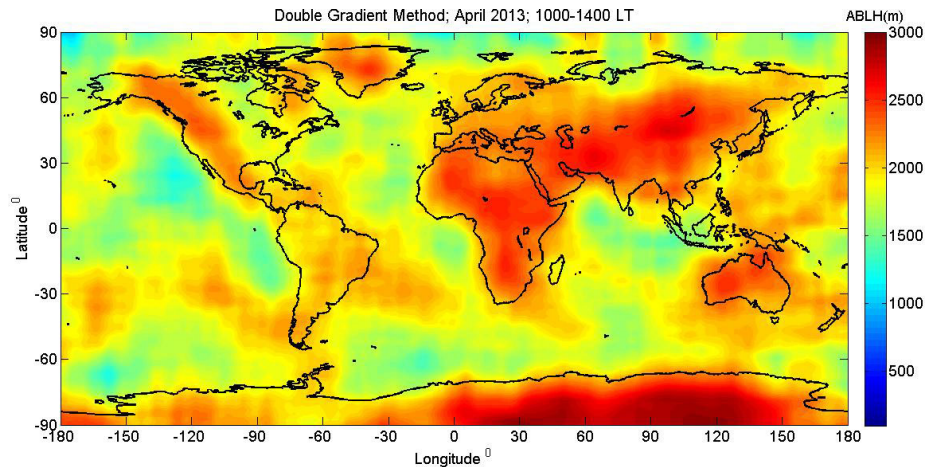


Figure 7b. Daytime (1000-1400 LT) trends of ABLH in March 2013, which are computed based on the Double Gradient Method (DGM).

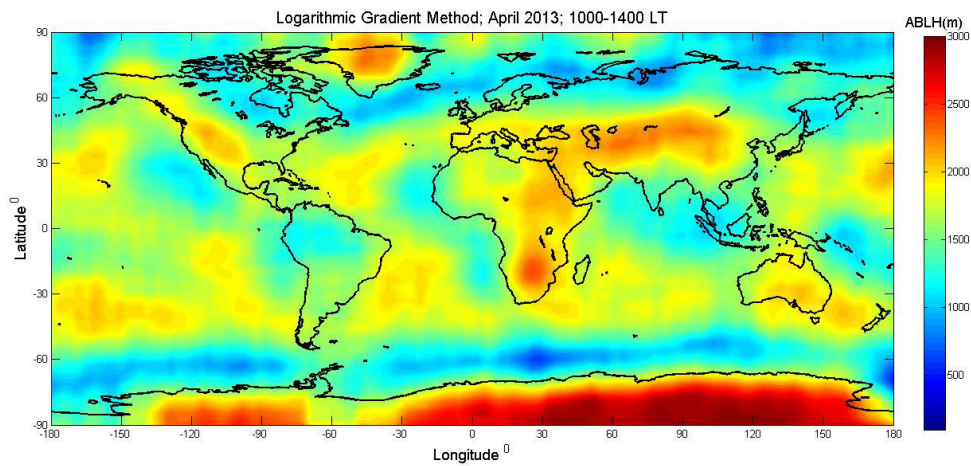


Figure 7c. Daytime (1000-1400 LT) trends of ABLH in March 2013, which are computed based on the Logarithmic Gradient Method (LGM).

3.2 Diurnal Variations

In order to verify the diurnal variations of ABLH, we present the local time vs. latitude variations in Figure 9 (a, b, c) during March and April 2013, respectively. Crystal clear diurnal variations can be seen, particularly, at sharp mid noon hours at both mid-latitude regions in northern (\sim between 20° N and 50° N) and southern (\sim between -20° S and -45° S) hemispheres, which almost resembles a Gaussian shape trend. No clear-cut diurnal variations can be found at equatorial regions. Further, relatively higher (\sim 2000 - 2500 meters) and consistent features, during both day and night times, are seen at the southern Polar Regions,

whereas relatively lower (less than 1000 meters) and consistent features can be seen at northern Polar Regions. It has been reported that ABLH variability is controlled by its diurnal cycle.¹² Further, it was reported that ABLH was too shallow (\sim 500 meters) at night (a stable layer), since the Earth's surface layer would become stable because of the infrared radiative cooling. On contrary, it shows deeper magnitudes in daytime hours (a convective layer) due to solar heating that would cause convective unstable conditions.¹¹ However, we do not find any early morning and evening transitions in ABLH which needs a more attention that would be tackled in the ensuing communication.

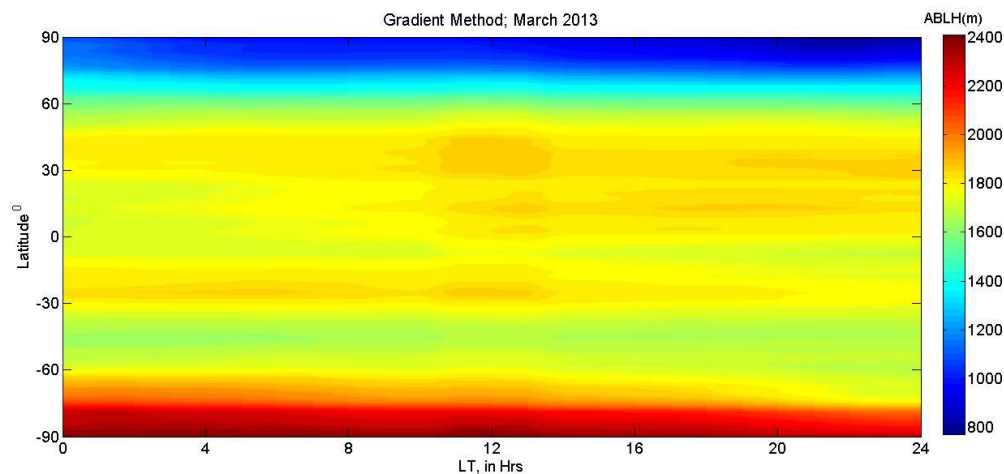


Figure 8a. Local time vs. Latitude variations of ABLH computed using the Gradient Method (GM) in March 2013.

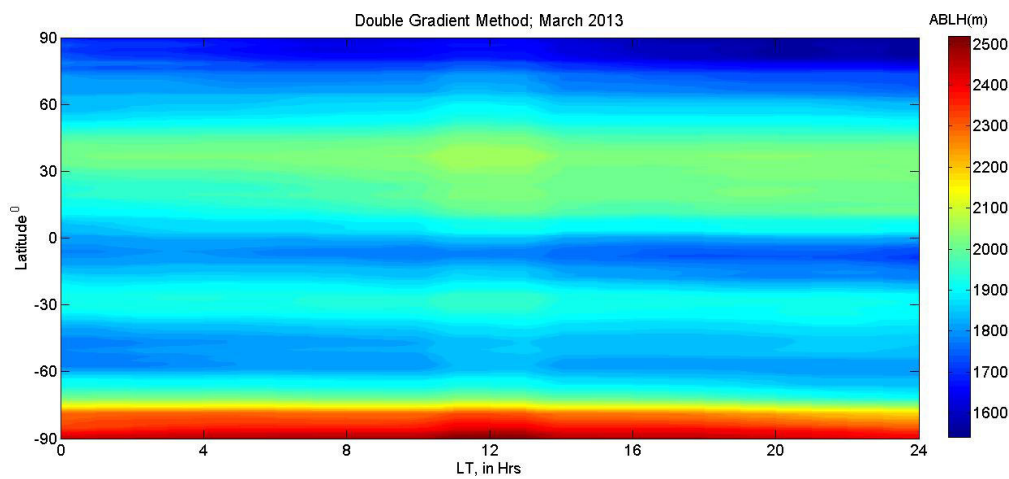


Figure 8b. Local time vs. Latitude variations of ABLH computed using the Double Gradient Method (DGM) in March 2013.

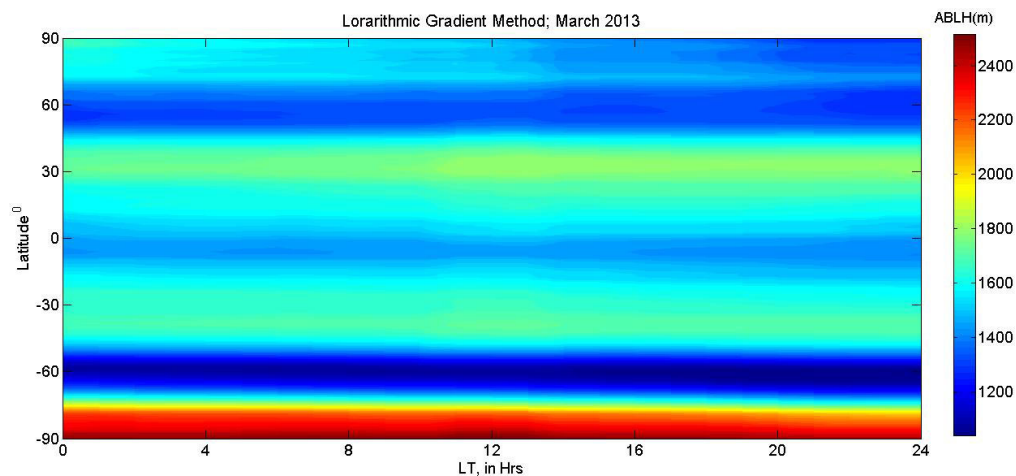


Figure 8c. Local time vs. Latitude variations of ABLH computed using the Logarithmic Gradient Method (LGM) in March 2013.

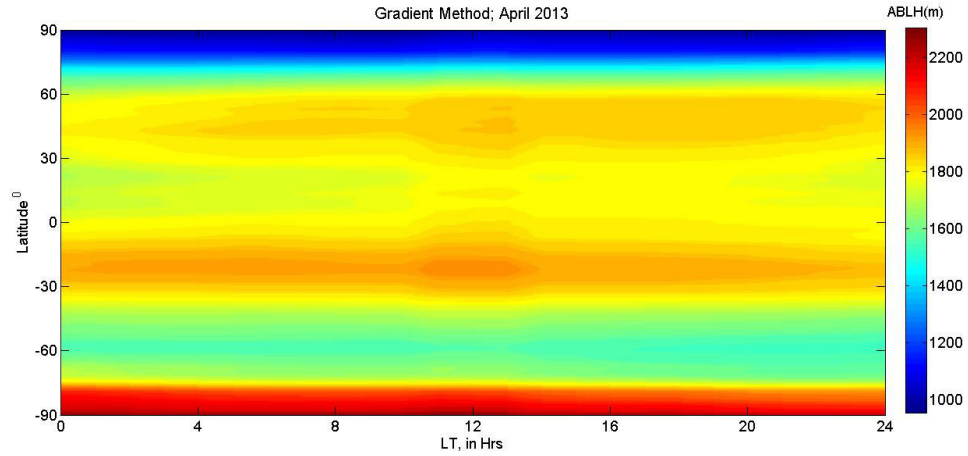


Figure 9a. Local time vs. Latitude variations of ABLH computed using the Gradient Method (GM) in April 2013.

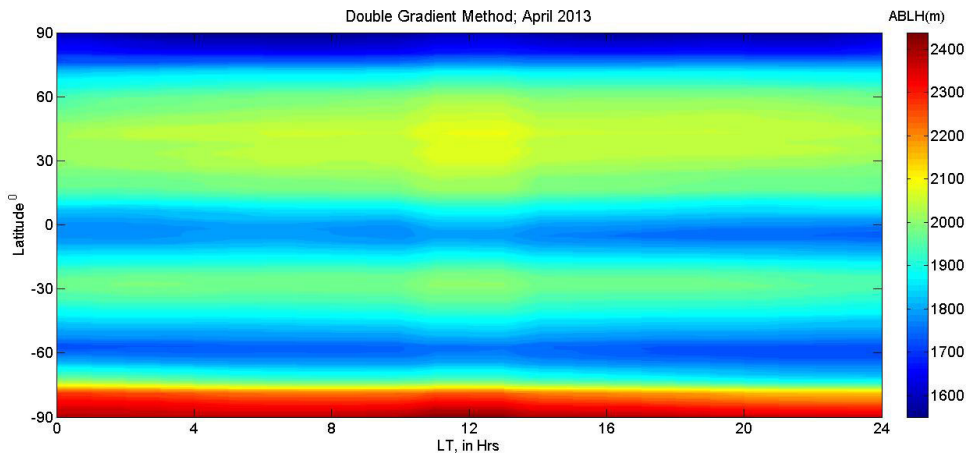


Figure 9b. Local time vs. Latitude variations of ABLH computed using the Double Gradient Method (DGM) in April 2013.

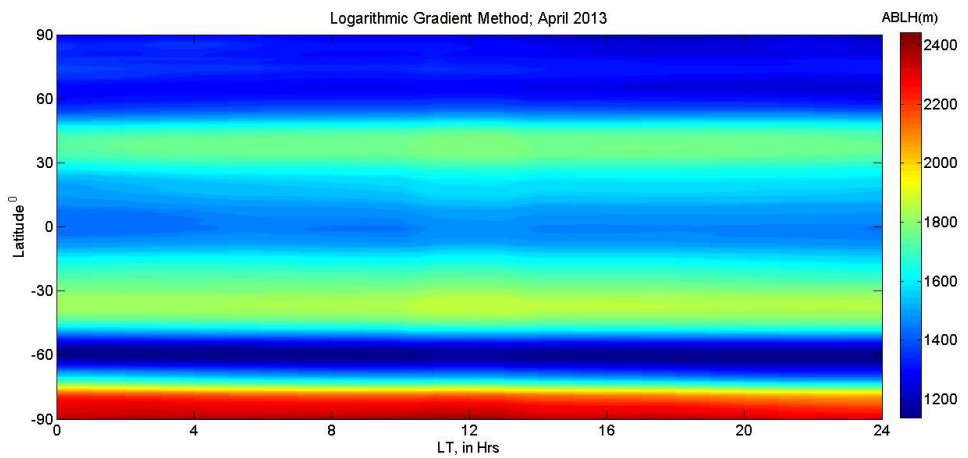


Figure 9c. Local time vs. Latitude variations of ABLH computed using the Logarithmic Gradient Method (LGM) in April 2013.

4. Future Studies

A future research will focus to verify the prowess of various methods (analytical, statistical and wavelet based technique) on huge databases available from the ensuing RO mission and individual station databases available from radiosonde instruments and micrometeorological towers.³³

5. Conclusion

In this study, we estimated ABLH using various analytical methods (gradient, double gradient and logarithmic gradient) by effectively utilizing COSMIC RO retrieved temperature profiles during March and April 2013 and presented both individual, global and diurnal features of ABLH. The observed research results are outlined hereunder:

- It is found that both gradient and logarithmic gradient methods show near-similar variations when compared to the double Gradient Method in estimating ABLH. It is, therefore, reported that double Gradient Method is not that much effective in ABLH studies when one utilizes COSMIC RO retrieved atmospheric products.
- Majority of land areas show higher ABLH during daytime hours (1000-1400 LT), which could happen when the Earth's surface temperatures are higher (an indication of the convective layer).
- Desert regions (Patagonian and Sahara) are associated with higher magnitudes during daytime hours, though a few fluctuations in higher magnitudes could be seen here and there (desert regions).
- Cold land regions (Arctic and Greenland regions) show too meager magnitudes (~500 meters only), whereas the Antarctic region depicts irregular structures and relatively higher magnitudes.
- Importantly, the majority of observational findings, as far as the global variations are concerned, is in great consistency with the climatology of ABLH derived using the ECMWF re-analysis.
- Diurnally a few distinctive features can be seen including, sharp peak at noon hours and lesser magnitudes in nighttime hours, which almost resembles a Gaussian shape trend.
- However, both early morning and evening transitions cannot be seen in the diurnal variations, and

- Diurnal variations are well captured by both gradient and logarithmic methods when compared to the double Gradient Method in estimating ABLH, which indicates the so-called double Gradient Method may not be suitable in estimating ABLH.

6. Acknowledgements

The logistic support of the Management of SVECW (Autonomous), Bhimavaram, Andhra Pradesh, India is highly acknowledged and appreciated, without which it could not have been possible to carry-out the present research. Temperature data downloaded from the COSMIC Data Analysis and Archive Center i.e., CDAAC (<http://cosmic-io.cosmic.ucar.edu/cdaac/index.html>).

7. References

1. Stull RB. An introduction to boundary layer meteorology. Dordrecht, Boston and London: Kluwer Academic Publishers; 1988. p. 1-666. <https://doi.org/10.1007/978-94-009-3027-8>
2. Garratt JR. The atmospheric boundary layer. Cambridge, U.K: Cambridge University Press; 1992; 14(2):112-3. PMID: PMC1882468.
3. Seibert P, Beyrich F, Gryning SE, Joffre S, Rasmussen A, Tercier P. Review and intercomparison of operational methods for the determination of the mixing height. *Atmospheric Environment*. 2000; 34(7):1001-27. [https://doi.org/10.1016/S1352-2310\(99\)00349-0](https://doi.org/10.1016/S1352-2310(99)00349-0)
4. Stevens B. Cloud-transitions and decoupling in shear-free stratocumulus-topped boundary layers. *Geophysical Research Letters*. 2002; 27(16):2557-60. <https://doi.org/10.1029/1999GL011257>
5. Lin, JT, Youn D, Liang XZ, Wuebbles DJ. Global model simulation of summertime U.S. ozone diurnal cycle and its sensitivity to PBL mixing, spatial resolution and emissions. *Atmos Environ*. 2008; 42:8470-83. <https://doi.org/10.1016/j.atmosenv.2008.08.012>
6. Pearson G, Davies F, Collier C. Remote sensing of the tropical rainforest boundary layer using pulsed Dopplerlidar. *Atmospheric Chemistry and Physics*. 2010; 10:5891-901. <https://doi.org/10.5194/acp-10-5891-2010>
7. Saha A, Mallet M, Roger JC, Dubuisson P, Piazzola J, Despiau S. One year measurements of aerosol optical properties over an urban coastal site: Effect on local direct radiative forcing. *Atmospheric Research*. 2008; 90(2-4):195-202. <https://doi.org/10.1016/j.atmosres.2008.02.003>
8. Ouwersloot HG, Vila-Gueraude Arellano J, Nolscher AC, Krol MC, Ganzeveld LN, Breitenberger C, Mammarella

- I, Williams J, Lelieveld J. Characterization of a boreal Convective Boundary Layer and its impact on atmospheric chemistry during HUMPPA-COPEC-2010. *Atmospheric Chemistry and Physics*. 2012; 12:9335–53. <https://doi.org/10.5194/acp-12-9335-2012>
9. Garratt JR. Review: The atmospheric boundary layer. *Earth-Science Reviews*. 1994; 37(1-2):89–134. [https://doi.org/10.1016/0012-8252\(94\)90026-4](https://doi.org/10.1016/0012-8252(94)90026-4)
 10. Seidel DJ, Ao CO, Li K. Estimating climatological planetary boundary layer heights from radiosonde observations: Comparison of methods and uncertainty analysis. *Journal of Geophysical Research*. 2010; 115(D16):113–3. <https://doi.org/10.1029/2009JD013680>
 11. Liu S, Liang X. Observed diurnal cycle climatology of planetary boundary layer height. *Journal of Climate*. 2010; 23(21):5790–809. <https://doi.org/10.1175/2010JCLI3552.1>
 12. Prijith SS, Rao PVN, Sujatha P, Dadhwal VK. Estimation of planetary boundary layer height using Suomi NPP-Cris soundings. *Remote Sensing Letters*. 2016; 7(7):621–30. <https://doi.org/10.1080/2150704X.2016.1171921>
 13. Angevine WM, White AB, Avery SK. Boundary-layer depth and entrainment zone characterization with a boundary-layer profiler. *Boundary Layer Meteorol*. 1994; 68(4):375–85. <https://doi.org/10.1007/BF00706797>
 14. Molod A, Salmun H, Dempsey M. Estimating planetary boundary layer heights from NOAA profiler network wind profiler data. *Journal of Atmospheric and Oceanic Technology*. 2015; 32:1545–61. <https://doi.org/10.1175/JTECH-D-14-00155.1>
 15. Davis KJ, Gamage N, Hagelberg CR, Kiemble C, Lenschow DH, Sullivan PP. An objective method for deriving atmospheric structure from airborne lidar observations. *Journal of Atmospheric and Oceanic Technology*. 2000; 17:1455–68. [https://doi.org/10.1175/1520-0426\(2000\)017<1455:AOMFDA>2.0.CO;2](https://doi.org/10.1175/1520-0426(2000)017<1455:AOMFDA>2.0.CO;2)
 16. Kumar YB. Portable lidar system for Atmospheric Boundary Layer measurements. *Optical Engineering*. 2006; 45(7):076201–5. <https://doi.org/10.1117/1.2221555>
 17. Guo P, Kuo YH, Sokolovskiy SV, Lenschow DH. Estimating Atmospheric Boundary Layer depth using cosmic radio occultation data. *Journal of Atmospheric Science*. 2011; 68:1703–13. <https://doi.org/10.1175/2011JAS3612.1>
 18. Ao CO, Mannucci, AJ, Kursinski ER. Improving GPS Radio Occultation stratospheric refractivity retrievals for climate benchmarking. *Geophysical Research Letters*. 2012; 39(12):1–18. <https://doi.org/10.1029/2012GL051720>
 19. Ho SP, Peng L, Anthes RA, Kuo YH, Lin HC. Marine boundary layer heights and their longitudinal diurnal and interannual variation in the southeast Pacific using COSMIC CALIOP and radiosonde data. *Journal of Climate*. 2015; 28(7):2856–72. <https://doi.org/10.1175/JCLI-D-14-00238.1>
 20. Von Engel A, Teixeira JA. Planetary boundary layer height climatology derived from ECMWF reanalysis data. *Journal of Climate*. 2013; 26(17):6575–90. <https://doi.org/10.1175/JCLI-D-12-00385.1>
 21. Liu J, Huang J, Chen B, Zhou T, Yan H, Jin H, Huang Z, Zhang B. Comparisons of PBL heights derived from CALIPSO and ECMWF reanalysis data over China. *Journal of Quantitative Spectroscopy and Radiative Transfer*. 2015; 153:102–12. <https://doi.org/10.1016/j.jqsrt.2014.10.011>
 22. Garfinkel CI, Waugh DW, Polvani LM. Recent Hadley cell expansion: The role of internal atmospheric variability in reconciling modeled and observed trends. *Geophysical Research Letter*. 2015; 42(24):10824–31. <https://doi.org/10.1002/2015GL066942>
 23. Babu N. Anomalous wind circulation over Taipei, Taiwan during the northern winter seasons of 2004 and 2005 - A case study. *Satellite Oceanography and Meteorology*. 2018; 3(2):01–11.
 24. Mastaan R, Brahmanandam PS, Uma G, Babu AN, Reddy KK. Studies of two important stability indices of Earth's atmosphere determined by using the COSMIC GPS Radio Occultation technique. *Indian Journal of Science and Technology*. 2016; 9(38):1–9. <https://doi.org/10.17485/ijst/2016/v9i38/98595>
 25. Brahmanandam PS, Chu YH, Liu J. Observations of equatorial Kelvin wave modes in FORMOSAT-3/COSMIC GPS RO temperature profiles. *Terrestrial Atmospheric and Oceanic Sciences*. 2010; 21(5):829–40. [https://doi.org/10.3319/TAO.2010.01.06.01\(A\)](https://doi.org/10.3319/TAO.2010.01.06.01(A))
 26. Ao CO, Hajj GA, Meehan TK, Dong D, Iijima BA, Mannucci AJ, Kursinski ER. Rising and setting GPS occultations by use of open-loop tracking. *Journal of Geophysical Research*. 2009; 21(5):829–40.
 27. Barbara H, Andrea L. Determination of the Atmospheric Boundary Layer height from radiosonde and lidar backscatter. *Boundary-Layer Meteorology*. 2006; 120(1):181–200. <https://doi.org/10.1007/s10546-005-9035-3>
 28. Shukla KK, Phanikumar DV, Newsom RK, Kumar KN, Ratnam MV, Naja M, Singh N. Estimation of the mixing layer height over a high altitude site in Central Himalayan region by using Doppler lidar. *Journal of Atmospheric and Solar-Terrestrial Physics*. 2014; 109:48–53. <https://doi.org/10.1016/j.jastp.2014.01.006>
 29. Yang T, Wang Z, Zhang W, Gbaguidi A, Sugimoto N, Wang Z, Matsui I, Sun Y. Technical note: Boundary layer height determination from lidar for improving air pollution episode modeling: Development of new algorithm and evaluation. *Atmospheric Chemistry and Physics*. 2017; 17:6215–25. <https://doi.org/10.5194/acp-17-6215-2017>
 30. Senff C, Bosenberg J, Peters G, Schaberl T. Remote sensing of turbulent ozone fluxes and the ozone budget in the

- Convective Boundary Layer with DIAL and radar-RASS: A case study. *Contributions to Atmospheric Physics*. 1996; 69(1):161–76.
31. Cheng CZF, Kuo YH, Anthes RA, Wu L. Satellite constellation monitors global and space weather. *Eos Transactions American Geophysical Union*. 2006; 87(17):166. <https://doi.org/10.1029/2006EO170003>
32. Angevine WM, Klein Baltink H, Bosveld FC. Observations of the morning transition of the convective boundary layer. *Boundary-Layer Meteorology*. 2001; 101(2):209–27. <https://doi.org/10.1023/A:1019264716195>
33. Sudarsan JS, Thattai D, Shah UK, Mitra A. Micrometeorological tower observations and their importance in atmospheric modeling and space technology. *Indian Journal of Science and Technology*. 2016 Nov; 9(42):1–6. <https://doi.org/10.17485/ijst/2016/v9i42/104594>